see commentary on page 1674

The connecting tubule is the main site of the furosemide-induced urinary acidification by the vacuolar H^+-ATPase

J Kovacikova[1], C Winter[1], D Loffing-Cueni[2], J Loffing[2,3], KE Finberg[4], RP Lifton[4], E Hummler[2], B Rossier[2] and CA Wagner[1]

[1]Institute of Physiology and Center for Integrative Human Physiology, University of Zurich, Zurich, Switzerland; [2]Department of Pharmacology and Toxicology, University of Lausanne, Lausanne, Switzerland; [3]Department of Medicine – Anatomy, University of Fribourg, Fribourg, Switzerland and [4]Department of Genetics, Yale Medical School, New Haven, Connecticut, USA

Final urinary acidification is achieved by electrogenic vacuolar H^+-ATPases expressed in acid-secretory intercalated cells (ICs) in the connecting tubule (CNT) and the cortical (CCD) and initial medullary collecting duct (MCD), respectively. Electrogenic Na^+ reabsorption via epithelial Na^+ channels (ENaCs) in the apical membrane of the segment-specific CNT and collecting duct cells may promote H^+-ATPases-mediated proton secretion by creating a more lumen-negative voltage. The exact localization where this supposed functional interaction takes place is unknown. We used several mouse models performing renal clearance experiments and assessed the furosemide-induced urinary acidification. Increasing Na^+ delivery to the CNT and CCD by blocking Na^+ reabsorption in the thick ascending limb with furosemide enhanced urinary acidification and net acid excretion. This effect of furosemide was abolished with amiloride or benzamil blocking ENaC action. In mice deficient for the IC-specific B1 subunit of the vacuolar H^+-ATPase, furosemide led to only a small urinary acidification. In contrast, in mice with a kidney-specific inactivation of the alpha subunit of ENaC in the CCD and MCD, but not in the CNT, furosemide alone and in combination with hydrochlorothiazide induced normal urinary acidification. These results suggest that the B1 vacuolar H^+-ATPase subunit is necessary for the furosemide-induced acute urinary acidification. Loss of ENaC channels in the CCD and MCD does not affect this acidification. Thus, functional expression of ENaC channels in the CNT is sufficient for furosemide-stimulated urinary acidification and identifies the CNT as a major segment in electrogenic urinary acidification.

Kidney International (2006) **70**, 1706–1716. doi:10.1038/sj.ki.5001851; published online 20 September 2006

KEYWORDS: H^+-ATPase; epithelial Na^+-channel; connecting tubule; furosemide; distal renal tubular acidosis (dRTA); mouse

Correspondence: *CA Wagner, Institute of Physiology and Center for Integrative Human Physiology, University of Zurich, Winterthurerstrasse 190, Zurich CH-8057, Switzerland. E-mail: Wagnerca@access.unizh.ch*

Received 2 January 2006; revised 28 June 2006; accepted 18 July 2006; published online 20 September 2006

The kidneys play a central role in maintaining acid–base homeostasis by reabsorbing bicarbonate and excreting acid equivalents generated by metabolism. Final urinary acidification takes place in the connecting tubule (CNT) and along the different segments of the collecting duct (CD) namely the cortical (CCD), outer medullary, and initial inner medullary collecting duct (MCD). These parts of the nephron are composed of segment-specific cells reabsorbing Na^+ and secreting K^+ and of intercalated cells (ICs) involved in acid–base transport. Many studies have described functionally and morphologically at least two types of ICs: type A and type B.[1–3] Type A ICs secrete protons via an apically expressed vacuolar H^+-ATPase.[4] This proton secretion is functionally coupled to the basolateral anion exchanger AE1 releasing bicarbonate into blood. Type B ICs reverse this process, thereby secreting bicarbonate into urine and absorbing protons.[1,5] The role of a third subtype, non-A/non-B ICs, is not fully clarified yet.

Proton secretion through vacuolar H^+-ATPases in the CNT and CCD is electrogenic and is thought to be indirectly coupled to Na^+ reabsorption.[4,6] Na^+ reabsorption through the amiloride-sensitive epithelial Na^+ channel (ENaC) expressed in neighboring segment-specific cells creates a more lumen-negative potential which has been hypothetized to enhance H^+ secretion by H^+-ATPases.[7–10] In the MCD, ENaC expression is much lower than in the CNT and CCD,[11] the lumen potential is more positive and H^+ secretion is independent from Na^+ absorption.[12]

The ENaC consists of three subunits termed α, β, γ.[13,14] Loss-of-function mutations in either the human α, β, or γ subunits of ENaC cause pseudohypoaldosteronism type 1 characterized by severe neonatal salt wasting, hyperkalemia, and metabolic acidosis.[15] The α subunit plays an essential role in the trafficking of the channel to the cell surface as well as forming part of the pore.[13] Apart from the kidney, ENaC is also expressed in distal colon and in upper and lower airways where it also mediates Na^+ reabsorption.[14] Mice with complete inactivation of αENaC develop acute postnatal respiratory distress and die within 40 h of birth from failure

to clear their lungs from liquid.[16] Recently, a novel mouse model has been generated with specific inactivation of αENaC in the entire CD but not in CNT,[17] providing a tool for studying sodium balance as well as disturbances of proton secretion secondary to defective Na^+ absorption.

The vacuolar H^+-ATPase is composed of at least 13 subunits of which several cell- and tissue-specific isoforms exist.[4,18,19] The B subunit forms part of the peripheral domain V_1 and two isoforms of this subunit, B1 and B2, have been identified. Whereas the B2 isoform (ATP6V1B2) is almost ubiquitously expressed and appears to serve in most cells a house-keeping function, the B1 isoform (ATP6V1B1) has a more limited tissue distribution: specialized cells of the epididymis,[20,21] the vas deferens,[21] the ciliary body of the eye,[22] the inner ear,[23] and all subtypes of ICs of the kidney.[20,24] Mutations in the gene encoding the B1 subunit result in distal renal tubular acidosis (dRTA) in man characterized by the inability of the distal nephron to appropriately acidify the urine.[23] A mouse model deficient for the *Atp6v1b1* gene has recently been generated with impaired urinary acidification.[25] Vacuolar H^+-ATPase activity is almost completely absent from the CCD. Interestingly, enhanced luminal appearance of the B2 subunit has been noted in B1-deficient ICs, suggesting that the B2 isoform could compensate for the loss of B1.[25] Nevertheless, *Atp6v1b1*-deficient mice develop a more severe metabolic acidosis with inappropriately alkaline urine when challenged with an oral acid-load (NH_4Cl) characteristic of dRTA.

Different subtypes of dRTA have been proposed and classified based on clinical tests.[26,27] These tests include oral NH_4Cl- or parenteral Na_2SO_4-loading and application of furosemide, which all lead to an acute urinary acidification in healthy subjects but not in patients with specific subtypes of dRTA. Furosemide inhibits the luminal $Na^+/K^+/2Cl^-$ cotransporter in the thick ascending limb, thereby increasing the delivered fraction of Na^+ to the subsequent nephron segments and stimulating Na^+ reabsorption through ENaC. Patients lacking an appropriate urinary acidification after furosemide application have been classified as suffering from the 'voltage-defective' form of dRTA.[9]

In order to test for and localize the possible functional interaction between Na^+ reabsorption and H^+ secretion in the different parts of the distal nephron, we performed clearance studies in mice treated acutely with furosemide, hydrochlorothiazide, and amiloride, and measured urinary acidification and net acid excretion (NAE).

RESULTS

Colocalization of vacuolar H^+-ATPase and ENaC in neighboring cells in the collecting system

Immunostaining of mouse kidney with antibodies against calbindin D28k, B1 subunit of the vacuolar H^+-ATPase, and the β subunit of the ENaC revealed that the B1 subunit of the H^+-ATPase is exclusively expressed in CNTs and CDs which were identified on account of their characteristic localization in the cortical labyrinth and the medullary rays, respectively, and by their strong labelling with antibodies against the beta subunit of the epithelial sodium channel (ENaC) and the calcium-binding protein calbindin D28k (Figure 1). Higher magnification showed that the B1 subunit is only expressed in a subtype of epithelial cells lining CNT and CD that do not express βENaC or calbindinD28k. This staining pattern is consistent with an exclusive localization of the B1 subunit in ICs[28,29] which are intermingled between the ENaC (and calbindin) positive CNT and CD (principal) cells.

The effect of furosemide and amiloride on urinary acidification

In a first group of control animals, the effect of acute furosemide and subsequent amiloride application on urinary

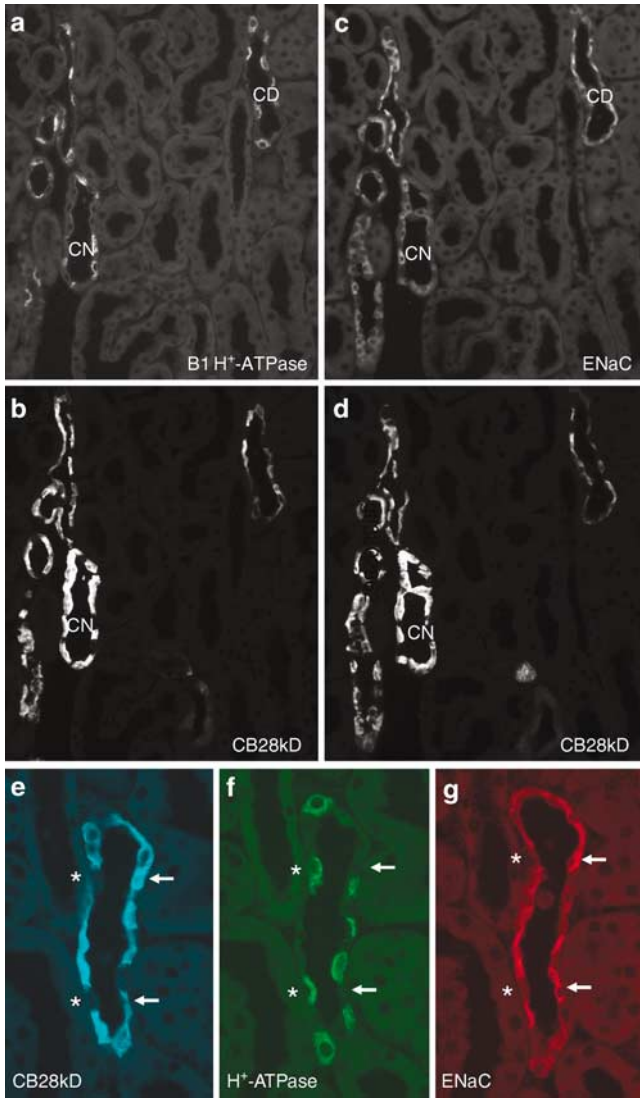

Figure 1 | Localization of vacuolar H^+-ATPases and the ENaC along the CNT and CCD in mouse kidney. (**a**–**d**) Consecutive mouse kidney sections (**a**/**b** and **c**/**d**) were stained against the B1 subunit of the vacuolar H^+-ATPase, the β subunit of the ENaC, and the calbindinD28k protein. Original magnification ×400. (**e**–**g**) Higher magnification of a CCD. ICs positive for the B1 subunit are marked with *, arrows indicate segment-specific cells stained for βENaC and calbindinD28k. Original magnification ×650.

acidification was tested. As shown in Figure 2a, the initial urinary pH was similar in all groups before the application of furosemide. A bolus of furosemide (2 μg/g of body weight (BW)) after 60 min lowered the urinary pH with being significantly more acidic after 90 min (furosemide: pH 6.16±0.08 versus control: pH 6.49±0.07), after 120 min (furosemide: pH 5.72±0.10 versus control: pH 6.39±0.08), and 150 min (furosemide: 5.63±0.084 versus control: pH 6.16±0.05). The furosemide-induced urinary acidification was completely abolished by the subsequent administration of amiloride or benzamil, inhibitors of ENaC activity: pH 6.09±0.09 in the furosemide+amiloride group versus 5.72±0.10 in furosemide-alone group after 120 min as well as after 150 min: pH 6.19±0.12 for furosemide+amiloride versus pH 5.63±0.08 for furosemide alone. The urine production and excretion remained stable in the control group during the entire experiment, whereas it increased in furosemide-treated animals from 1.9±0.3 μl/g after 60 min to 5.2±0.8 μl/g after 90 min. A similar effect was observed in mice treated subsequently with amiloride, resulting in an increase in urine output from 3.0±0.6 μl/g BW after 60 min to 6.5±0.7 μl/g BW after 90 min. (Figure 2b). The analysis of urinary electrolyte excretion revealed that the fractional excretion (FE in %) of sodium and chloride increased in mice treated with furosemide plus amiloride (Figure 2d and e) with a maximum after 120 min (FE of sodium 1.67±0.31% for furosemide+amiloride versus 0.25±0.08% in control and FE of chloride 2.29±0.38% in furosemide+amiloride versus 0.70±0.24% in control). As summarized in Table 1 and Figure 3, furosemide treatment resulted in a slightly decreased blood potassium concentration (4.8±0.3 mmol/l in furosemide versus 5.7±0.2 mmol/l in control) and augmented blood bicarbonate concentration (21.0±0.7 with furosemide versus 19.7±1.0 mmol/l under control).

Thus, treatment of mice with furosemide led to the expected increase in urinary output with an increase in fractional sodium and potassium excretion accompanied by a strong urinary acidification as described previously for rats and humans.[9] The stimulation of urinary acidification was abolished by the ENaC inhibitors amiloride and benzamil

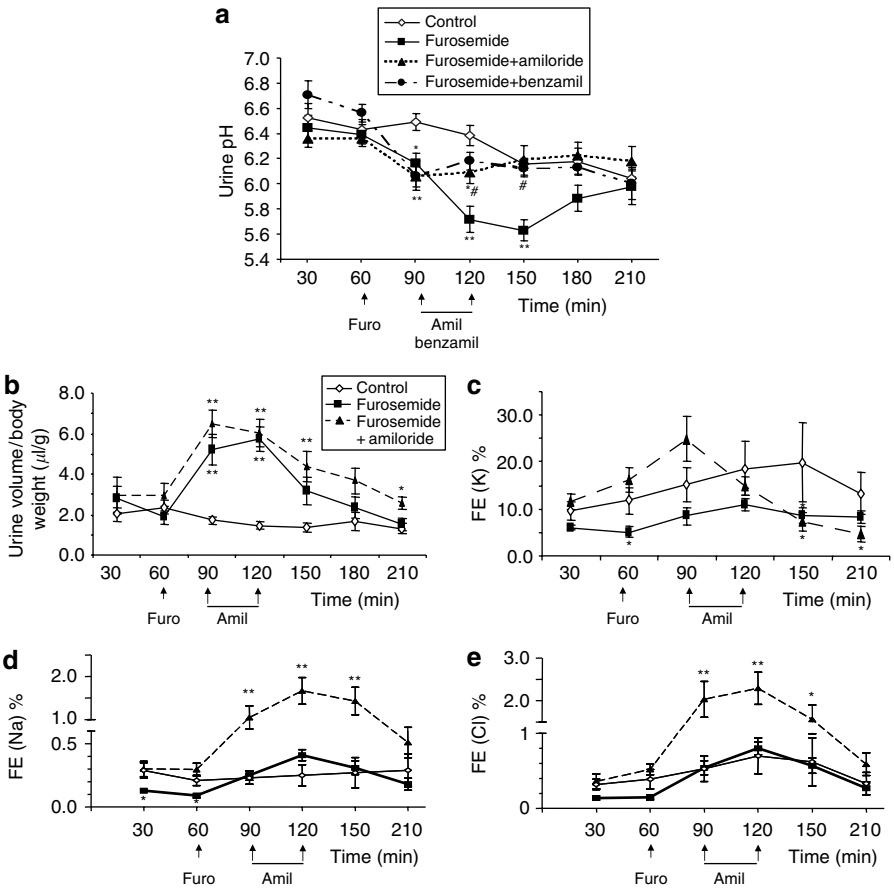

Figure 2 | Effect of furosemide and amiloride on urinary pH and electrolyte excretion. (**a**) Application of furosemide (2 μg/g BW) ($n=17$) caused acidification of urinary pH compared to untreated wild-type mice (*Atp6v1b1* +/+, $n=13$). The effect of furosemide on urine pH was reversed in mice treated subsequently with amiloride (5 μg/g BW) ($n=14$) or benzamil (2 μg/g BW) ($n=6$). (**b**) Urine production and excretion remained stable in the control group during the experiment, whereas it increased in furosemide- and amiloride-treated animals. (**c**) The FE (%) of potassium increased in furosemide-treated animals and was reversed by the addition of amiloride. (**d**, **e**) The FE % of sodium and chloride showed an increase of both electrolytes in the furosemide- and amiloride-treated animals. $^{*}P<0.05$ and $^{**}P<0.001$ versus control, $^{\#}P<0.05$ between furosemide treatment and furosemide+benzamil/furosemide+amiloride.

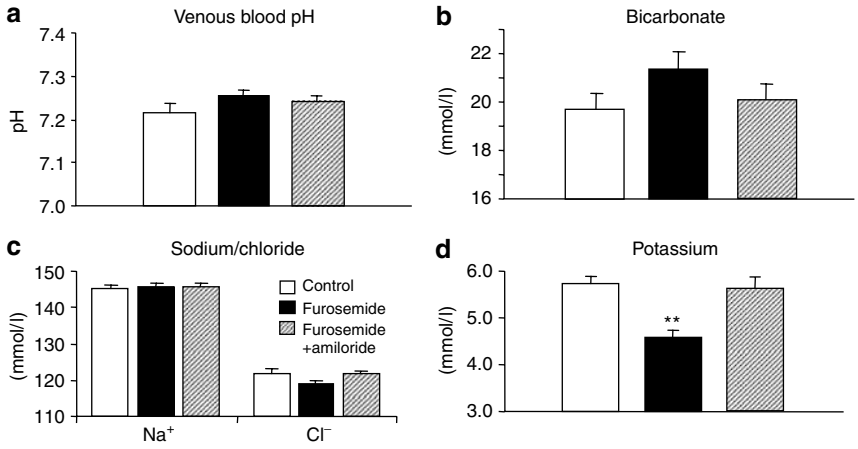

Figure 3 | Effect of furosemide and amiloride on blood pH and electrolytes. (**a–d**) Furosemide treatment resulted in decreased blood potassium concentration as expected from the increased urinary excretion. Blood bicarbonate levels showed a tendency to be higher which did not reach statistical significance. $^{**}P<0.001$ versus control.

consistent with a role of ENaC in the furosemide-induced urinary acidification. A similar effect of amiloride and the structurally unrelated ENaC blocker triamterene on the furosemide-induced urinary acidification has also been reported in rats.[30]

The furosemide-induced urinary acidification is reduced in mice deficient for the IC-specific vacuolar H^+-ATPase B1 subunit (ATP6V1B1)

To demonstrate that the furosemide-induced urinary acidification depended on the activity of vacuolar H^+-ATPases localized in ICs, we used a mouse model deficient for the IC-specific B1 subunit (*Atp6v1b1* −/−). *Atp6v1b1* −/− furosemide-treated mice exhibited a markedly higher basal urine pH than the *Atp6v1b1* +/+ furosemide-treated mice (pH 7.19±0.16 versus 6.44±0.10) and only a mild urinary acidification upon furosemide administration could be observed: pH 6.86±0.15 versus 5.72±0.10 after 120 min (Figure 4a). The residual urinary acidification observed in the B1-deficient mice may be owing to a partial compensation by the B2 isoform which is more luminally localized in ICs of *Atp6v1b1* −/− mice.[25] To assess the effect of the treatments on NAE, we measured total NH_3/NH_4^+ and total phosphate excretion in urine and estimated NAE from these data as the urine samples were too small to measure titratable acidity. Both total NH_3/NH_4^+ and total phosphate excretion increased in response to furosemide as described previously in rats.[30] Application of furosemide increased NAE from 2.9±0.3 mmol/l/mg/dl creatinine in control animals to 6.2±0.6 mmol/l/mg/dl creatinine (Figure 4b). In mice given amiloride, NAE showed a tendency to be lower ($P=0.08$). In contrast, in benzamil-treated mice and in the B1-deficient mice, NAE was significantly lower (benzamil: 3.7±0.6 mmol/l/mg/dl creatinine, B1 KO: 4.4±0.4 mmol/l/mg/dl creatinine).

Atp6v1b1 −/− furosemide-treated mice also had a strikingly higher urine output than the *Atp6v1b1* +/+ furosemide-treated mice after 60 min before the furosemide administration: 3.2±0.83 μl/g BW versus 1.9±0.34 μl/g BW (Figure 4c). Furosemide administration led to a more profound diuresis in *Atp6v1b1* −/− mice: 8.9±1.0 μl/g BW versus 5.2±0.7 μl/g BW after 90 min (Figure 4c). In addition, *Atp6v1b1* −/− mice had a significantly lower basal FE of potassium than *Atp6v1b1* +/+ mice (1.89±0.24 versus 6.09±0.60%) (Figure 4d), basal FE of sodium (0.06±0.01 versus 0.13±0.01%) (Figure 4e), and basal FE of chloride (0.04±0.01 versus 0.14±0.01%) (Figure 4f) pointing to a defect in urine concentration. Furosemide administration further revealed a significant difference in the FE of potassium, whereas the FE of sodium and chloride did not differ between *Atp6v1b1* −/− and *Atp6v1b1* +/+ mice (Figure 4e and f). As summarized in Table 1 and Figure 5, analysis of blood electrolytes revealed differences in potassium and bicarbonate levels.

The CD-specific loss of αENaC expression in Scnn1a^{loxloxCre} mice does not affect the furosemide-induced urinary acidification and diuretic response

Scnn1a^{loxloxCre} mice lack the alpha subunit of the ENaC in the CCD and MCD but not in the connecting segment.[17] We used these mice to test for the furosemide-stimulated urinary acidification. Basal urine output, urine pH, and electrolyte content were not significantly different between control mice (*Scnn1a*^{loxlox}) and mice with the specific ablation of αENaC expression (*Scnn1a*^{loxloxCre}) (compare Tables 1 and 2). Furosemide administration caused urinary acidification in both genotypes to a similar extent: *Scnn1a*^{loxlox} and *Scnn1a*^{loxloxCre} mice: pH 6.00±0.10 versus 5.89±0.09 after 120 min (Figure 6a). Also, estimated NAE at the time point 150 min was similar in both groups of mice (Figure 6b; Scnn1a^{loxlox} 5.4±0.9 mmol/l/mg/dl creatinine versus Scnn1a^{loxloxCre} 4.2±0.6 mmol/l/mg/dl creatinine, $P=0.31$). No difference between *Scnn1a*^{loxlox} and *Scnn1a*^{loxloxCre} mice in urine output could be detected (7.9±1.9 μl/g BW versus 8.2±1.1 μl/g BW after 90 min.) (Figure 6c). Furosemide also failed to unmask a possible difference between *Scnn1a*^{loxlox}

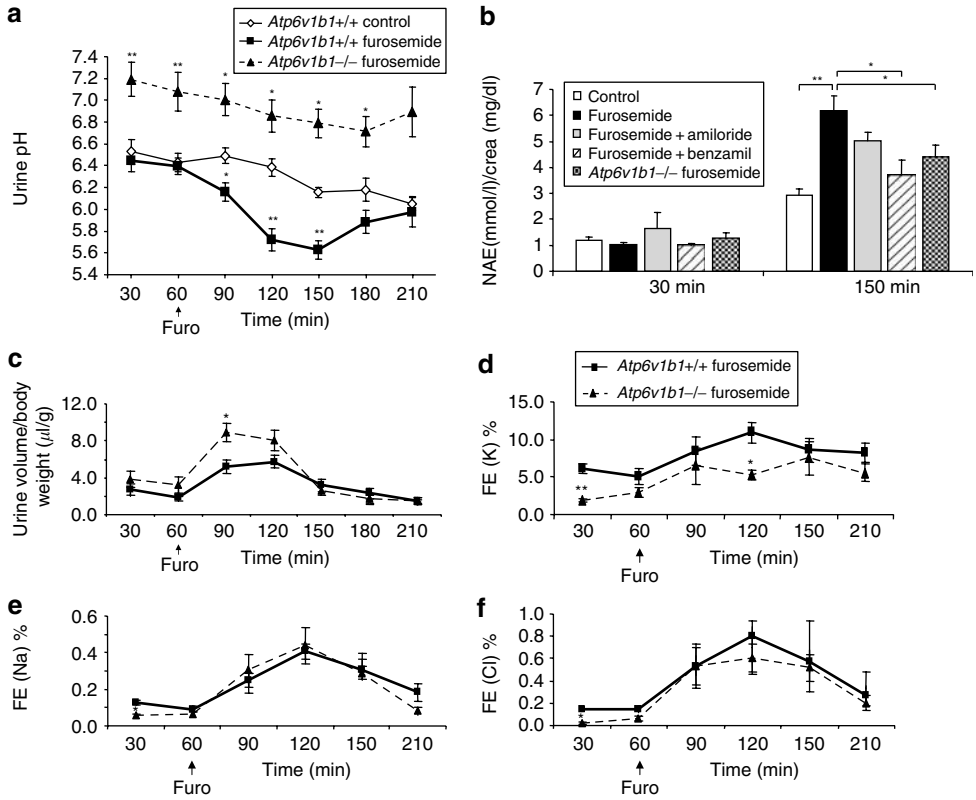

Figure 4 | Effect of furosemide on urine pH and electrolyte excretion in mice deficient for the B1 vacuolar H^+-ATPase subunit (*Atp6v1b1* −/−). (**a**) *Atp6v1b1* −/− received furosemide (2 µg/g BW) ($n = 9$) and urine pH acidified only mildly. $^{**}P < 0.001$ versus control. (**b**) Estimated NAE at the time point 30 min and 150 min. NAE increased after furosemide application and the rise in NAE was significantly reduced after application of benzamil and in the *Atp6v1b1*-deficient mice ($^{*}P < 0.05$ significant difference between furosemide-treated animals and other groups). (**c**) Furosemide administration led to a more profound diuresis in *Atp6v1b1* −/− in comparison to *Atp6v1b1* +/+ mice. (**d–f**) The FE of Na^+ and Cl^- was similar in both genotypes; however, the FE % for potassium was lower in B1-deficient mice. Values of control and furosemide-treated animals from Figure 2 are shown again for comparison. $^{*}P < 0.05$ and $^{**}P < 0.001$ versus *Atp6v1b1* +/+ treated with furosemide.

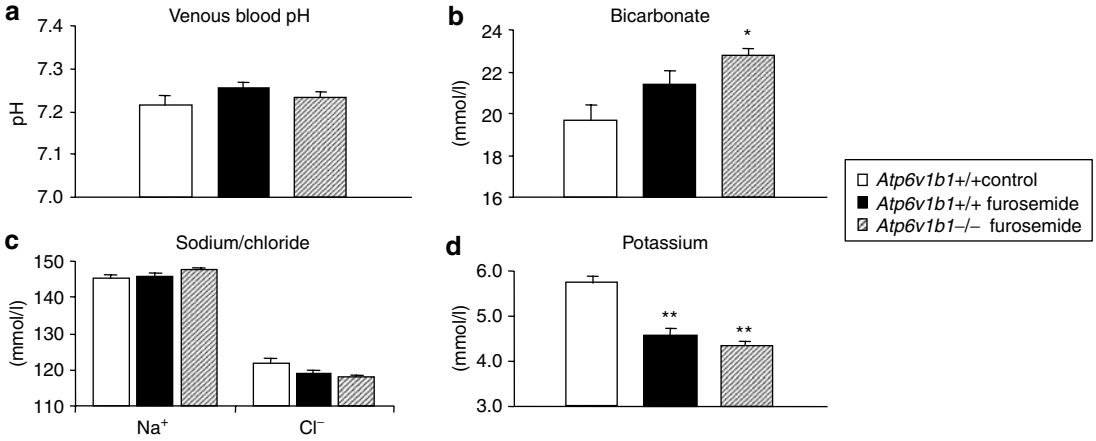

Figure 5 | Effect of furosemide on blood pH and electrolytes in *Atp6v1b1* −/− mice. (**a–d**) Blood potassium levels were also lower in B1-deficient mice after treatment with furosemide. Bicarbonate was higher than in untreated wild-type animals. Values from wild-type animals are shown again in Figure 3 for comparison. $^{*}P < 0.05$ and $^{**}P < 0.001$ versus control.

and *Scnn1a*^{loxloxCre} mice in the FE of sodium: 1.87 ± 0.42% versus 2.13 ± 0.54% after 120 min (Figure 6e and Table 2). However, blood electrolyte analysis revealed a significantly lower blood bicarbonate concentration (23.5 ± 0.7 mmol/l in *Scnn1a*^{loxlox} versus 21.3 ± 0.7 mmol/l in *Scnn1a*^{loxloxCre} (Table 2 and Figure 7b). Thus, after application of furosemide, no significant difference was found in the diuretic response, urinary acidification, and electrolyte excretion suggesting

Table 1 | Summary of blood pH, gas, and electrolytes of wild-type mice left untreated (control) and wild-type and Atp6V1b1-deficient mice treated with furosemide and amiloride at the end of the experimental period

	Atp6v1b1 +/+ control	*Atp6v1b1* +/+ furosemide	*Atp6v1b1* +/+ furosemide amiloride	*Atp6v1b1* −/− furosemide
pH	7.22 ± 0.02	7.24 ± 0.02	7.24 ± 0.02	7.25 ± 0.04
pCO_2 (mmHg)	50.6 ± 3.9	50.8 ± 2.0	47.7 ± 2.1	53.8 ± 7.4
HCO_3^- (mmol/l)	19.7 ± 1.0	21.0 ± 0.7	19.8 ± 0.4	21.8 ± 1.6*
K^+ (mmol/l)	5.7 ± 0.2	4.8 ± 0.3**	5.5 ± 0.2	4.3 ± 0.1**
Na^+ (mmol/l)	145.5 ± 0.8	147.7 ± 0.9	145.4 ± 0.5	147.6 ± 1.4
Cl^- (mmol/l)	121.8 ± 1.5	120.9 ± 0.8	121.1 ± 0.8	119.6 ± 2.4
Serum creatinine (mg/dl)	0.14 ± 0.02	0.11 ± 0.01	0.13 ± 0.02	0.12 ± 0.01
Weight (g)	27.5 ± 1.5	29.6 ± 1.1	25.4 ± 1.1	24.6 ± 1.0
CrCl/BW 30 min (μl/min/g)	18.3 ± 4.2	33.4 ± 6.1	15.6 ± 4.9	28.5 ± 6.0
CrCl/BW 90 min (μl/min/g)	18.7 ± 4.7	44.6 ± 8.5*	19.0 ± 3.4	26.6 ± 5.6
CrCl/BW 120 min (μl/min/g)	13.8 ± 3.9	33.2 ± 4.6**	22.1 ± 7.0	20.3 ± 9.2
NH_3/NH_4^+ (mM)/creatinine (mg/dl), 30 min	1.04 ± 0.05	0.94 ± 0.08	1.47 ± 0.52	1.18 ± 0.15
NH_3/NH_4^+ (mM)/creatinine (mg/dl), 150 min	1.40 ± 0.0.18	2.60 ± 0.08	2.04 ± 0.08	2.56 ± 0.26
NAE (mM/creatinine (mg/dl), 30 min	1.21 ± 1.11	1.03 ± 0.07	1.63 ± 0.64	1.29 ± 0.20
NAE (mM/creatinine (mg/dl), 150 min	2.91 ± 0.28	6.16 ± 0.59	5.02 ± 0.33	4.40 ± 0.44*

BW, body weight; CrCl, creatinine clearance; NAE, net acid excretion.
*Marks significant differences $P < 0.05$, **$P < 0.001$.

Table 2 | Summary of blood pH, gas, and electrolytes of *Scnn1a*^{loxlox} and *Scnn1a*^{loxloxCre} mice deficient for the alpha ENaC subunit treated with furosemide and hydrochlorothiazide

	Scnn1a^{loxlox} furosemide	*Scnn1a*^{loxloxCre} furosemide	*Scnn1a*^{loxlox} furosemide HCT	*Scnn1a*^{loxloxCre} furosemide HCT
pH	7.28 ± 0.02	7.28 ± 0.03	7.33 ± 0.03	7.25 ± 0.03
PCO_2 (mmHg)	51.4 ± 2.2	47.3 ± 3.1	43.9 ± 4.9	55.4 ± 2.1*
HCO_3^- (mmol/l)	23.5 ± 0.7	21.3 ± 0.7*	21.9 ± 0.9	23.3 ± 1.3
K^+ (mmol/l)	4.4 ± 0.2	4.4 ± 0.3	4.5 ± 0.2	4.9 ± 0.2
Na^+ (mmol/l)	147.8 ± 0.9	147.8 ± 0.7	147.6 ± 0.8	148.0 ± 0.5
Cl^- (mmol/l)	119.9 ± 1.8	120.2 ± 1.3	114.2 ± 1.5	114.6 ± 1.6
Serum creatinine (mg/dl)	0.15 ± 0.02	0.11 ± 0.01	0.14 ± 0.03	0.13 ± 0.02
Weight (g)	25.4 ± 1.9	24.9 ± 1.2	33.6 ± 1.7	29.9 ± 1.9
CrCl/BW 30 min (μl/min/g)	14.4 ± 3.4	21.7 ± 3.3	24.15 ± 6.3	29.0 ± 4.4
CrCl/BW 90 min (μl/min/g)	21.5 ± 3.7	20.8 ± 2.7	21.6 ± 3.0	22.4 ± 4.1
CrCl/BW 120 min (μl/min/g)	10.5 ± 2.0	13.9 ± 2.2	12.8 ± 1.7	13.4 ± 2.4
NH_3/NH_4^+ (mM)/creatinine (mg/dl), 30 min	1.25 ± 0.30	1.47 ± 0.73		
NH_3/NH_4^+ (mM)/creatinine (mg/dl), 150 min	2.24 ± 0.36	1.82 ± 0.24		
NAE (mM/creatinine (mg/dl), 30 min	1.46 ± 0.32	1.93 ± 0.70		
NAE (mM/creatinine (mg/dl), 150 min	5.41 ± 0.90	4.25 ± 0.60		

BW, body weight; CrCl, creatinine clearance; NAE, net acid excretion.
*Marks significant differences $P < 0.05$, **$P < 0.001$.

that preserved expression of αENaC in the CNT is sufficient to maintain the furosemide-induced urinary acidification.

In order to inhibit a possible compensatory increase in Na^+ absorption in the distal tubule via the thiazide-sensitive Na^+/Cl^- cotransporter, furosemide was applied together with hydrochlorothiazide. Figure 8a shows that the urinary pH of *Scnn1a*^{loxloxCre} mice did not differ significantly from the urine pH of *Scnn1a*^{loxlox} mice before furosemide and hydrochlorothiazide (furo + HCT) administration. After administration of furosemide together with hydrochlorothiazide (furo + HCT), *Scnn1a*^{loxloxCre} mice decreased their urine pH to the same extent as the *Scnn1a*^{loxlox} mice: pH 5.77 ± 0.12 versus pH 5.66 ± 0.10 after 120 min. Urine output, fractional electrolyte excretion and systemic electrolyte, and blood gas status were not distinguishable between both mouse lines (Figures 8 and 9 and Table 2).

DISCUSSION

In the present study, we investigated the functional interaction between renal Na^+ reabsorption through ENaC and H^+ secretion by vacuolar H^+-ATPases in the connecting segment and CCD. Both ENaC and vacuolar H^+-ATPases containing the B1 subunit isoform are expressed together in the same nephron segments, namely CNT and CCD in neighboring cells. H^+ secretion by vacuolar H^+-ATPases is electrogenic and thought to be indirectly coupled to Na^+ reabsorption.[31] According to this hypothesis, Na^+ reabsorption through ENaC creates a more lumen-negative transtubular voltage which in turn would enhance H^+ secretion by vacuolar H^+-ATPases. Thus, the furosemide-induced increase in Na^+ delivery to the CNT and CCD and the subsequent reabsorption of this delivered fraction through ENaC may result in urinary acidification mediated by vacuolar H^+-ATPases.

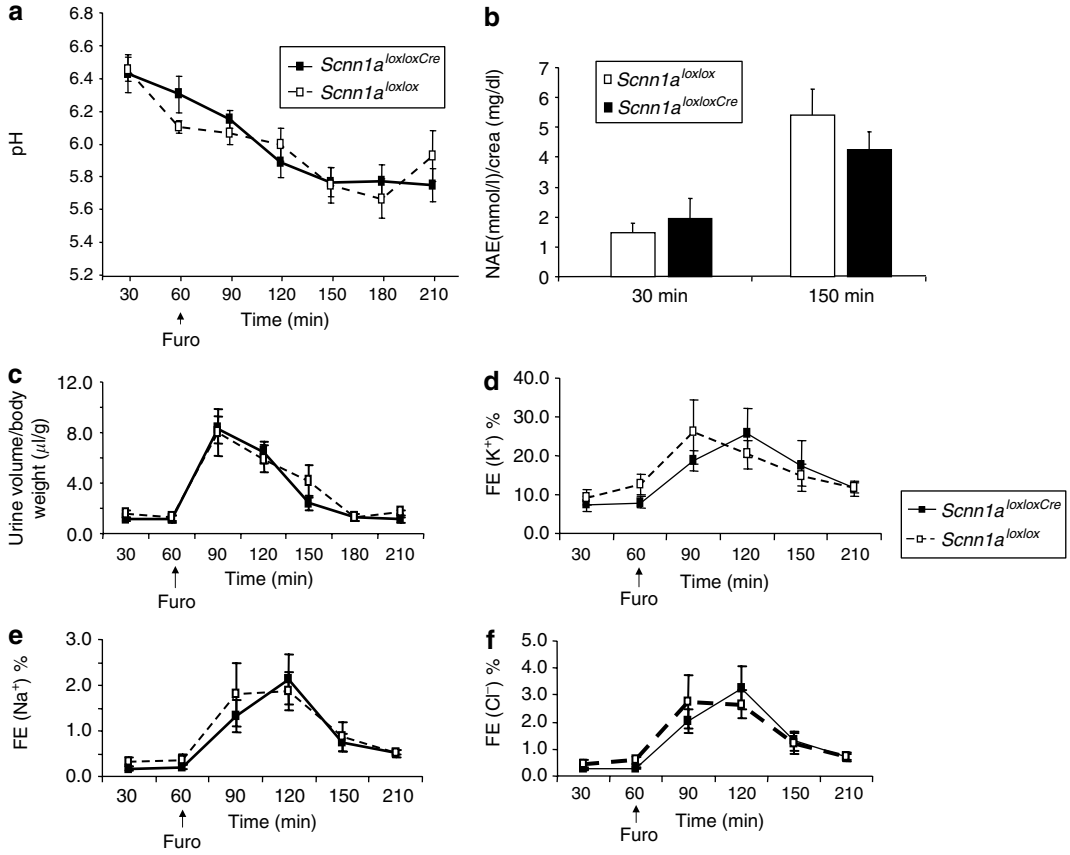

Figure 6 | Effect of furosemide on urine pH and electrolyte excretion in *Scnn1a*^{loxlox} and *Scnn1a*^{loxloxCre} mice. (**a**) The effect of furosemide on urinary acidification in *Scnn1a*^{loxlox} ($n=10$) and *Scnn1a*^{loxloxCre} ($n=12$) mice. Furosemide administration did not show any difference in urine pH between *Scnn1a*^{loxlox} and *Scnn1a*^{loxloxCre} mice. (**b**) No difference in the furosemide-induced increase in the estimated rate of NAE was observed between *Scnn1a*^{loxlox} and *Scnn1a*^{loxloxCre} treated with furosemide. (**c**) Urine volume/BW in *Scnn1a*^{loxlox} ($n=11$) and *Scnn1a*^{loxloxCre} ($n=10$) mice. No difference between *Scnn1a*^{loxlox} and *Scnn1a*^{loxloxCre} mice in urine output was reported. (**d**–**f**) FE of potassium, sodium, and chloride in *Scnn1a*^{loxlox} ($n=6$) and *Scnn1a*^{loxloxCre} ($n=7$) mice. Furosemide-induced increase of FE of potassium, sodium, and chloride did not differ between *Scnn1a*^{loxlox} and *Scnn1a*^{loxloxCre} mice.

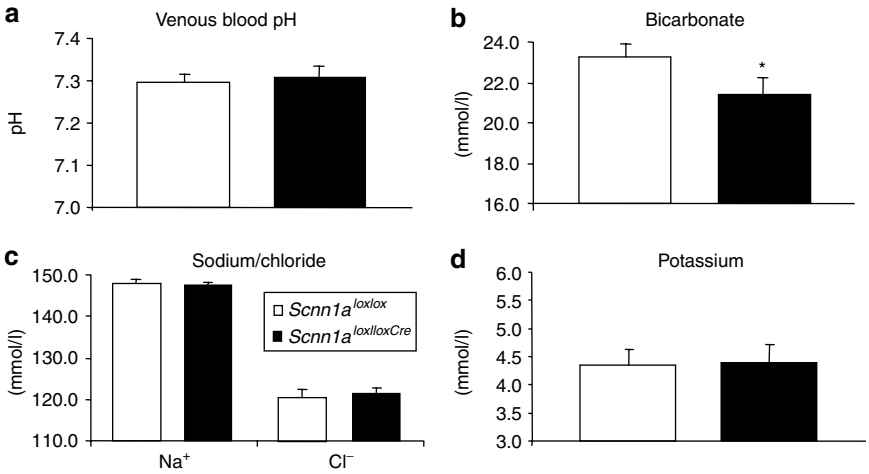

Figure 7 | Effect of furosemide on blood pH and electrolytes in *Scnn1a*^{loxlox} and *Scnn1a*^{loxloxCre} mice. *Scnn1a*^{loxloxCre} mice had a significantly lower bicarbonate concentration. Other parameters were not different. *$P<0.05$ versus *Scnn1a*^{loxlox}.

Several types of defects in distal renal tubular acidification have been classified based on provocative tests using infusions containing sulfate, bicarbonate, or phosphate, oral NH_4Cl loading or furosemide application and the respective response in urinary pH, net acid, and electrolyte excretion as well as the ability to sustain a blood–urine PCO_2 gradient.[32] At least three types of dRTA have been distinguished, a 'secretory type' with a defect supposed in the proton-secretory proton pumps, a

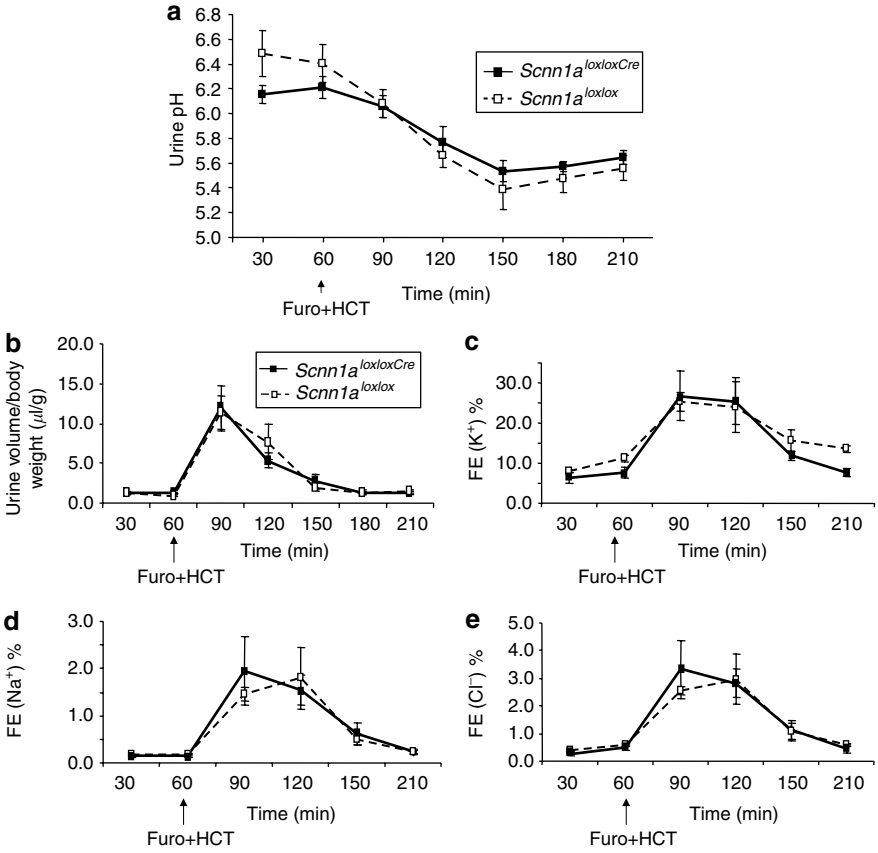

Figure 8 | (a) Effect of furosemide (2 µg/g BW) and hydrochlorothiazide (HCT, 0.05 µg/g BW) on urinary acidification in *Scnn1a*^{loxlox} ($n = 6$) and *Scnn1a*^{loxloxCre} ($n = 6$) mice. Urine pH of *Scnn1a*^{loxloxCre} mice did not differ significantly from the urine pH of *Scnn1a*^{loxlox} mice neither before nor after furosemide + HCT administration. (**b**–**e**) Urine output and FE of potassium, sodium, and chloride in furosemide- and hydrochlorothiazide-treated *Scnn1a*^{loxlox} ($n = 5$) and *Scnn1a*^{loxloxCre} ($n = 7$) mice. No difference between *Scnn1a*^{loxlox} and *Scnn1a*^{loxloxCre} mice in urine output, FE of potassium, sodium, and chloride was reported.

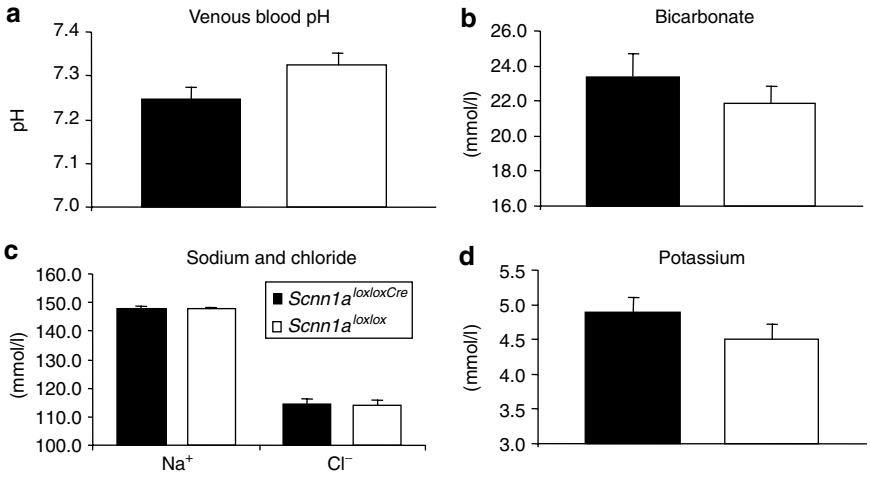

Figure 9 | Blood pH and electrolytes in furosemide- and hydrochlorothiazide-treated *Scnn1a*^{loxlox} ($n = 5$) and *Scnn1a*^{loxloxCre} ($n = 7$) mice. No significant difference between *Scnn1a*^{loxlox} *and Scnn1a*^{loxloxCre} mice in blood pH and electrolytes could be observed.

'back-leak type' where H^+ or HCO_3^- may leak back, and a 'voltage-defective type' where the inability to produce an acid urine may result from the failure to produce a favorable lumen-negative potential facilitating proton secretion.[9,26,33] Consistent with these functional classifications, application of amiloride to patients and experimental animals reduces urinary proton secretion.[9,32,34] LiCl has been used as another tool to induce the voltage-dependent defect; however, several

studies have indicated that the defects induced by LiCl and amiloride are different.[35] The defect induced by administration of LiCl can be restored by Na_2SO_4 infusion[32] and is associated with altered expression levels of H^+/K^+-ATPases and H^+-ATPases.[36]

In our experiments, furosemide induced a strong urinary acidification. This acidification apparently depends on the activity of vacuolar H^+-ATPases containing the B1 isoform as no or only a mild acidification could be observed in *Atp6v1b1* deficient mice. Thus, vacuolar H^+-ATPases are the main mediator of the furosemide-induced urinary acidification. The result also suggests that H^+/K^+-ATPases, the other potential acid-secretory pumps, do not play an important role as an acid-secretory mechanism under these experimental conditions. However, we observed a lower urinary potassium excretion in the B1-deficient mice. The mechanism is presently unknown. A stimulation of H^+/K^+-ATPases, potentially induced by a higher urinary flow rate, could contribute to this effect.

The effect of furosemide was blunted by amiloride inhibiting ENaC-dependent Na^+ absorption as evident from the increased fractional Na^+ excretion and decreased fractional K^+-excretion. In a separate group of animals, the consequence of the genetic ablation of ENaC channel function was tested in *Scnn1a*^{loxloxCre} mice. These animals lack the alpha subunit of ENaC which is essential for ENaC function and results in no detectable ENaC channel function and loss of luminal localization of beta and gamma subunits in the CCD and outer medullary CD.[17] In the CNT, however, ENaC function and localization has remained normal.[17] In the control and αENaC-deficient mice, furosemide induced normal urinary acidification with a similar increase in fractional Na^+, Cl^-, and K^+ excretion. In order to rule out a compensatory increase in Na^+ absorption by the thiazide-sensitive Na^+/Cl^- cotransporter, we also tested for the combined effect of furosemide and hydrochlorothiazide which caused a stronger urinary acidification and diuretic response to the same extent in both groups of animals. Thus, the furosemide-induced urinary acidification involves the activity of an amiloride- and benzamil-sensitive mechanism, most likely ENaC. In view of the normal capacity of *Scnn1a*^{loxloxCr} mice to reabsorb Na^+ and to respond to furosemide and hydrochlorothiazide, it appears that the residual ENaC function in the CNT may be sufficient for the furosemide-induced urinary acidification. However, it cannot be completely ruled out that amiloride acts also on a mechanism distinct from ENaC and that this mechanism is still operative in the *Scnn1a*^{loxloxCre} mice. Based on mathematical modelling of transport processes involved in acid secretion and electrolyte transport along the CD, it has been recently proposed that the generation of a more lumen-negative potential by the action of ENaC could hardly account for changes in vacuolar H^+-ATPase activity.[7] Weinstein[7] argued that the change in transtubular voltage is minor compared to the ability of the pump to be active even against a larger voltage gradient, and proposed that amiloride interacts also with other mechanisms. These calculations were made for the CCD and may not fully apply for the CNT which was identified here as the main target of furosemide. However, our results do not completely rule out that some of the urinary acidification induced by furosemide took place in the CCD and that amiloride acted on a mechanism distinct from ENaC. This mechanism, however, remains to be identified and local opposing pH gradients must also be taken into consideration. In addition, Hropot *et al.*[30] reported that the structurally unrelated triamterene has a similar inhibitory effect on the furosemide-induced urinary acidification strongly suggesting that ENaC is the common target.

This identifies the CNT as the major segment mediating furosemide-induced urinary acidification. Similar conclusions have been reached with respect to the Na^+-absorbing capacity of the CNT versus CCD.[17] Further experiments establishing a complete genetic ablation of αENaC expression along the entire CNT and CD will be helpful to prove this hypothesis.

In summary, the furosemide-induced urinary acidification requires vacuolar H^+-ATPases containing the B1 subunit, is inhibited by amiloride, and is not altered in a mouse model with preserved ENaC function in the CNT but loss of ENaC function in the CCD and outer medullary collecting duct. The results point to a hitherto unrecognized major role of the CNT in electrogenic H^+-secretion and the urinary acidification induced by furosemide.

MATERIALS AND METHODS

Animals

Experiments were performed on *Atp6v1b1* +/+ and *Atp6v1b1* −/− mice[25]) and *Scnn1a*^{loxloxCre} and *Scnn1a*^{loxlox} mice.[17] They were maintained on a standard diet and had a free access to drinking water. All experiments were performed according to Swiss Animal Welfare laws and approved by the Local Veterinary Authority.

The generation, breeding, and genotyping of *Atp6v1b1*−/−, *Scnn1a*^{loxlox}, and *Scnn1a*^{loxloxCre} has been described previously.[17,25]

Blood and urinary parameters

Mice were anesthetized intraperitoneally (ketamine 1 μl/g BW and xylazine 1 μl/g BW), placed on a heated table maintained at 37°C and a catheter was placed into the urinary bladder. Urine was collected every 30 min during the whole period of 3.5 h for the measurement of urine volume, pH, sodium, chloride, potassium, and creatinine concentrations. To prevent dehydration, mice were constantly supplemented with 125 mM NaCl and 25 mM $NaHCO_3$ (pH 7.4) according to their urinary output. At the end of the experiment, heparinized mixed venous blood was collected for the measurement of pH, blood gases, sodium, potassium, chloride, and creatinine concentrations. After an initial recovery phase and collection of a baseline value at 30 min, at 60 min *Atp6v1b1* +/+, *Atp6v1b1* −/−, *Scnn1a*^{loxlox}, and *Scnn1a*^{loxloxCre} mice were administered furosemide 2 μg/g BW subcutaneously; some of the *Scnn1a*^{loxlox} and *Scnn1a*^{loxloxCre} mice were also given hydrochlorothiazide 0.05 μg/g BW together with furosemide. Two subgroups of *Atp6v1b1* +/+ mice received additionally amiloride 5 μg/g BW subcutaneously or benzamil 2 μg/g BW subcutaneously after 90 and 120 min of the experiment. All drugs were finally dissolved in

125 mM NaCl + 25 mM $NaHCO_3$. Control mice received only 125 mM NaCl + 25 mM $NaHCO_3$.

Urinary pH was immediately measured; urine and blood electrolytes and other blood parameters (pCO_2, pO_2) were determined using a blood gas analyzer (ABL 505, Radiometer, Copenhagen, Denmark). Urinary creatinine was measured by the Jaffe method. Serum creatinine was determined by an enzymatic reaction (F DAOS method, Wako Creatinine F L-Type kit, Wako Chemicals GmbH, Germany). Total urinary NH_3/NH_4^+ was measured using the Berthelot protocol,[37] total urinary phosphate using a commercial kit (Sigma, Buchs, Switzerland). NAE was estimated from the concentration of total NH_3/NH_4^+, total phosphate as the major titratable acid, and urine pH using the Henderson–Hasselbalch equation and assuming blood pH 7.4.

Immunohistochemistry

Fixation of mouse kidneys and tissue processing for immunohistochemistry was performed as described previously.[28] Consecutive cryosections (4–5 μm thick) of the fixed kidneys were placed on chrom-alum gelatine-coated slides, preincubated with 10% normal goat serum in phosphate-buffered saline, and afterwards incubated overnight at 4°C with mouse-anti-chicken calbindin D28k antibodies (Swant Bellinzona, Switzerland, dilution 1/20 000 in phosphate-buffered saline-1% bovine serum albumin) that was applied together with either rabbit-anti-rat βENaC antisera[17] (dilution 1/1000 in phosphate-buffered saline-1% bovine serum albumin) or rabbit-anti-rabbit B1 subunit of H^+-ATPase[20] (dilution 1/1000 in phosphate-buffered saline-1% bovine serum albumin). Binding sites of the primary antibodies were revealed with fluorescein isothiocynate-coupled goat-anti-mouse immunoglobulin G and Cy3-coupled goat-anti-rabbit immunoglobulin G (both from Jackson Immuno Research Laboratories, West Grove, PA, USA).

Statistical analysis

All data were tested for statistical analysis using paired and unpaired Student's *t*-tests and analysis of variance, and only data with $P < 0.05$ were considered statistically significant. A minimum of 6–8 animals was used for each measurement and treatment.

ACKNOWLEDGMENTS

The study has been supported by grants from the Swiss National Research foundation to CA Wagner (31-068318) and J Loffing (3200B0-105769/1) and the University Research Priority Program 'Integrative Human Physiology' of the University of Zurich. We acknowledge the technical assistance of Nicole Fowler-Jaeger.

REFERENCES

1. Schuster VL. Function and regulation of collecting duct intercalated cells. *Annu Rev Physiol* 1993; **55**: 267–288.
2. Kim J, Kim YH, Cha JH *et al.* Intercalated cell subtypes in connecting tubule and cortical collecting duct of rat and mouse. *J Am Soc Nephrol* 1999; **10**: 1–12.
3. Alper SL, Natale J, Gluck S *et al.* Subtypes of intercalated cells in rat kidney collecting duct defined by antibodies against erythroid band 3 and renal vacuolar H^+-ATPase. *Proc Natl Acad Sci USA* 1989; **86**: 5429–5433.
4. Wagner CA, Finberg KE, Breton S *et al.* Renal vacuolar H^+-ATPase. *Physiol Rev* 2004; **84**: 1263–1314.
5. Wagner CA, Geibel JP. Acid-base transport in the collecting duct. *J Nephrol* 2002; **5**(suppl): S112–S127.
6. Koeppen BM, Helman SI. Acidification of luminal fluid by the rabbit cortical collecting tubule perfused *in vitro*. *Am J Physiol* 1982; **242**: F521–F531.
7. Weinstein AM. A mathematical model of rat collecting duct III. Paradigms for distal acidification defects. *Am J Physiol Renal Physiol* 2002; **283**: F1267–F1280.
8. Weinstein AM. A mathematical model of rat collecting duct I. Flow effects on transport and urinary acidification. *Am J Physiol Renal Physiol* 2002; **283**: F1237–F1251.
9. Batlle DC. Segmental characterization of defects in collecting tubule acidification. *Kidney Int* 1986; **30**: 546–554.
10. Chang H, Fujita T. A numerical model of acid–base transport in rat distal tubule. *Am J Physiol Renal Physiol* 2001; **281**: F222–F243.
11. Loffing J, Kaissling B. Sodium and calcium transport pathways along the mammalian distal nephron: from rabbit to human. *Am J Physiol Renal Physiol* 2003; **284**: F628–F643.
12. Jacobsen HJ, Furuya H, Breyer MD. Mechanism and regulation of proton transport in the outer medullary collecting duct. *Kidney Int* 1991; **40**: S51–S56.
13. Kellenberger S, Schild L. Epithelial sodium channel/degenerin family of ion channels: a variety of functions for a shared structure. *Physiol Rev* 2002; **82**: 735–767.
14. Rossier BC, Pradervand S, Schild L *et al.* Epithelial sodium channel and the control of sodium balance: interaction between genetic and environmental factors. *Annu Rev Physiol* 2002; **64**: 877–897.
15. Lifton RP, Gharavi AG, Geller DS. Molecular mechanisms of human hypertension. *Cell* 2001; **104**: 545–556.
16. Hummler E, Barker P, Gatzy J *et al.* Early death due to defective neonatal lung liquid clearance in alpha-ENaC-deficient mice. *Nat Genet* 1996; **12**: 325–328.
17. Rubera I, Loffing J, Palmer LG *et al.* Collecting duct-specific gene inactivation of alphaENaC in the mouse kidney does not impair sodium and potassium balance. *J Clin Invest* 2003; **112**: 554–565.
18. Nelson N, Harvey WR. Vacuolar and plasma membrane proton-adenosinetriphosphatases. *Physiol Rev* 1999; **79**: 361–385.
19. Nishi T, Forgac M. The vacuolar (H+)-ATPases – nature's most versatile proton pumps. *Nat Rev Mol Cell Biol* 2002; **3**: 94–103.
20. Finberg KE, Wagner CA, Stehberger PA *et al.* Molecular cloning and characterization of *Atp6v1b1*, the murine vacuolar H^+-ATPase B1-subunit. *Gene* 2003; **318**: 25–34.
21. Breton S, Smith PJ, Lui B, Brown D. Acidification of the male reproductive tract by a proton pumping (H^+)-ATPase. *Nat Med* 1996; **2**: 470–472.
22. Wax MB, Saito I, Tenkova T *et al.* Vacuolar H^+-ATPase in ocular ciliary epithelium. *Proc Natl Acad Sci USA* 1997; **94**: 6752–6757.
23. Karet FE, Finberg KE, Nelson RD *et al.* Mutations in the gene encoding B1 subunit of H^+-ATPase cause renal tubular acidosis with sensorineural deafness. *Nat Genet* 1999; **21**: 84–90.
24. Nelson RD, Guo XL, Masood K *et al.* Selectively amplified expression of an isoform of the vacuolar H^+-ATPase 56-kilodalton subunit in renal intercalated cells. *Proc Natl Acad Sci USA* 1992; **89**: 3541–3545.
25. Finberg KE, Wagner CA, Bailey MA *et al.* The B1 subunit of the H^+ATPase is required for maximal urinary acidification. *Proc Nat Acad Sci USA* 2005; **102**: 13616–13621.
26. Arruda JA, Kurtzman NA. Mechanisms and classification of deranged distal urinary acidification. *Am J Physiol* 1980; **239**: F515–F523.
27. DuBose Jr TD, Alpern RJ. Renal tubular acidosis. In: Scriver CR, Beaudet AL, Sly WS, Valle D (eds). *The Metabolic and Molecular Bases of Inherited Disease*, 8th edn, McGraw-Hill: New York, 2001, pp 4983–5021.
28. Loffing J, Loffing-Cueni D, Valderrabano V *et al.* Distribution of transcellular calcium and sodium transport pathways along mouse distal nephron. *Am J Physiol Renal Physiol* 2001; **281**: F1021–F1027.
29. Biner HL, Arpin-Bott MP, Loffing J *et al.* Human cortical distal nephron: distribution of electrolyte and water transport pathways. *J Am Soc Nephrol* 2002; **13**: 836–847.
30. Hropot M, Fowler N, Karlmark B *et al.* Tubular action of diuretics: distal effects on electrolyte transport and acidification. *Kidney Int* 1985; **28**: 477–489.
31. Hamm LL, Alpern RJ. Cellular mechanisms of renal tubular acidification. In: Seldin DW, Giebisch G (eds). *The Kidney: Physiology and Pathophysiology*, 3rd edn, Lippincott Williams & Wilkins: Philadelphia, 2000, pp 1935–1979.
32. DuBose Jr TD, Caflisch CR. Validation of the difference in urine and blood carbon dioxide tension during bicarbonate loading as an index of distal nephron acidification in experimental models of distal renal tubular acidosis. *J Clin Invest* 1985; **75**: 1116–1123.

33. Batlle D, Flores G. Underlying defects in distal renal tubular acidosis: new understandings. *Am J Kidney Dis* 1996; **6**: 896–915.
34. Kornandakieti C, Tannen RL. H^+ transport by the aldosterone-deficient rat distal nephron. *Kidney Int* 1984; **25**: 629–635.
35. Mehta PK, Sodhi B, Arruda JA, Kurtzman NA. Interaction of amiloride and lithium on distal urinary acidification. *J Lab Clin Med* 1979; **93**: 983–994.
36. Eiam-Ong S, Dafnis E, Spohn M *et al.* H-K-ATPase in distal renal tubular acidosis: urinary tract obstruction, lithium, and amiloride. *Am J Physiol* 1993; **265**: F875–F880.
37. Quentin F, Chambrey R, Trinh-Trang-Tan MM *et al.* The Cl^-/HCO_3^- exchanger pendrin in the rat kidney is regulated in response to chronic alterations in chloride balance. *Am J Physiol Renal Physiol* 2004; **287**: F1179–F1188.